RESEARCH ARTICLE

SAMRIDDHI Volume 12, Issue 1, 2020 Print ISSN: 2229-7111 Online ISSN: 2454-5767

Determination of Residual Stresses in Ceramic-Metal Brazed Joint using Finite Element Analysis and Experimental Validation of the Results

Dheeraj Kumar Sharma[1,2*], Mainak Bandyopadhyay[1,4], Jaydeep Joshi[1], Arun K. Chakraborty[1,3]

[1]Scientific Officer, Institute for Plasma Research, Bhat, Gandhinagar-382428, Gujarat, India

[2]MSc Scholar, Homi Bhabha National Institute (HBNI), Anushaktinagar, Mumbai-400094, Maharashtra, India

[3]Assistant Project Director, ITER-India, Institute for Plasma Research, Koteshwar, Ahmedabad-380005, Gujarat, India

[4]Scientific Officer, ITER-India, Institute for Plasma Research, Koteshwar, Ahmedabad-380005, Gujarat, India

Abstract

Ceramic vacuum feedthroughs are an inevitable requirement for any vacuum system, which requires electrical feedlines to be inserted into the vacuum environment. These feedthroughs consist of metal-ceramic-metal transition and, therefore, require the brazing process as a joining technique. This process allows joining two base materials, i.e., Alumina and Kovar, for this case, which manifests different thermo-mechanical response. The difference between the coefficient of thermal expansion (CTE) of these materials causes the development of residual stresses during the cooling phase of the brazing process. Such residual stresses, if not addressed properly, can lead to the failure in the brazed joint even before the design limits. The purpose of this study is to assess these stresses by performing the thermo-mechanical analysis of the brazing process of ceramic-metal assembly through finite element analysis (FEA) technique. This study includes the assessment of non-linear behavior (due to temperature-dependent material properties) of Alumina and Kovar assembly. Further, X-ray diffraction (XRD) based residual stress measurement technique has been utilized to validate the FEA results. The paper shall present the FEA methodology (model, boundary condition, and results) followed by the experimental results and their comparison.

Keywords: Alumina, Brazing, Ceramic feedthroughs, CTE, Kovar, Residual stresses, Thermo-mechanical analysis, Vacuum, XRD.

SAMRIDDHI: A Journal of Physical Sciences, Engineering and Technology (2020); DOI: 10.18090/samriddhi.v12i01.1

Introduction

Ceramic vacuum feedthroughs are essential requirements for machines, like ITER,[1] where the electrical penetrations from air to high vacuum environments are a necessity. Such feedthroughs are subjected to high vacuum, high voltage, and high radiation (neutron and gamma) environment. Because of these hostile environments, ceramic feedthroughs are to be manufactured with quality to withstand the requirements. However, to mount/connect these feedthroughs, metallic transitions are needed at both ends of the ceramic material, as shown as an example in Figure 1.

To join ceramic and metal for making a hermetic seal, a vacuum brazing technique[2,3] is used. Joining of dissimilar materials using brazing introduces residual stresses in the assembly due to the fact of the differential coefficient of thermal expansion. Therefore, the thermo-mechanical characterization of the brazed joint is an essential parameter to be established to ensure safe and sound design.

In this paper, the FEA of Alumina-Kovar brazed sample is carried out for the brazing process with brazing alloy as TiCuSil. The brazed sample is analyzed only for the cool down cycle of the brazing process as during the heating cycle of the brazing, all parts are free to expand as they are not constrained. When the brazed joint is cooled down from the solidus temperature of the braze alloy to the room temperature, there are significant stresses developed at the joint since the interface is constrained due to bonding. For the realistic results, temperature-dependent non-linear

Corresponding Author: Dheeraj Kumar Sharma, Institute for Plasma Research, Bhat, Gandhinagar-382428, Gujarat, India, e-mail: dheeraj@ipr.res.in

How to cite this article: Sharma, D. K., Bandyopadhyay, M., Joshi, J., & Chakraborty, A. K. (2020). Determination of residual stresses in ceramic-metal brazed joint using Finite Element Analysisand experimental validation of the results. *SAMRIDDHI: A Journal of Physical Sciences, Engineering and Technology, 12*(1), 1-7.

Source of support: Nil

Conflict of interest: None

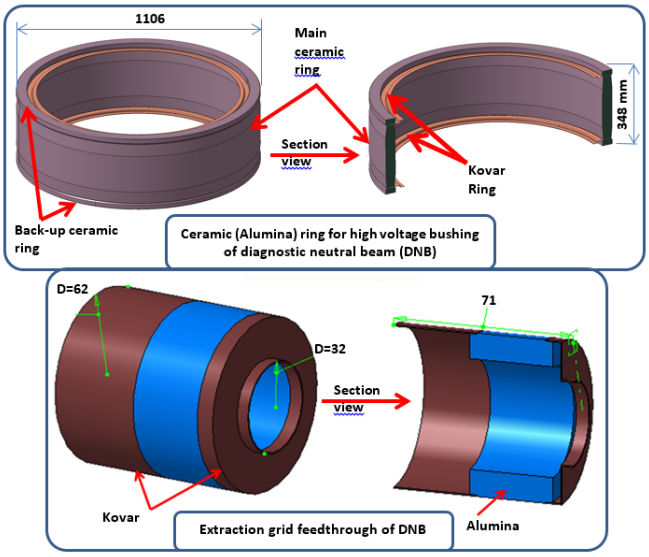

Figure 1: Few examples of brazed electrical ceramic feedthroughs used in ITER-DNB system (all dimensions are in mm)

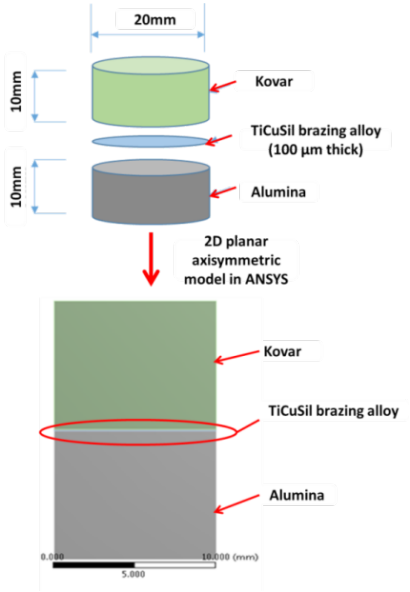

Figure 2: Finite element (FE) model geometry

material properties and plasticity behavior of brazing alloy are taken into consideration as plastic behavior of brazing alloy is expected to relax the stresses. For experimental validation of the FEA results, the sample of the same material was manufactured following the same thermal cycle, and the residual stresses were assessed using XRD.

Finite Element Analysis (FEA) Model and Non-linear Material Properties

Problem Setup in ANSYS

For the simulation, the cylindrical butt joint of Alumina, Kovar, and brazing alloy (TiCuSil) is used, as illustrated in Figure 2.

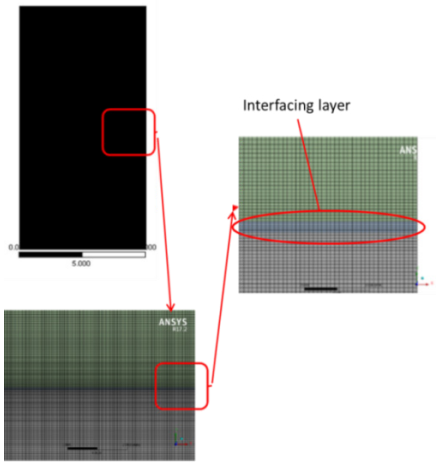

Figure 3: Meshed FE model

Due to cylindrical geometry, a 2D planar axisymmetric model is created in ANSYS. To capture the plasticity effect, brazing alloy, 100 microns thickness, sandwiched between Alumina and Kovar disks is modeled. The condition of axisymmetric ensures a very less number of mesh elements, and so the calculation time, without compromising the accuracy or calculation efficiency by the software, as compared to the complete 3D model.

Meshing of Finite Element (FE) Model

Mesh is composed of quadrilateral elements. Biasing is given to the mesh to have high mesh density, as shown in Figure 3, of elements at the interface location to capture the details of the thin braze alloy layer (which is merely 100 microns thick). Two-dimensional structural plane elements "PLANE 183" are used to perform the analysis, which has the axisymmetric feature to accommodate the requirement. As the analysis is performed for the cooling cycle only, the contacts between Kovar, the braze alloy, and Alumina are considered bonded with the plasticity behavior of the brazing alloy.

Non-Linear Material Properties

To predict the residual stresses quantitatively, it is important to incorporate the temperature-dependent non-linear material properties of all the parts used in the assembly into the FEA model. In this case, 780°C (braze alloy solidus temperature) to ambient is the temperature range considered for the study.

The material properties of the ceramic disk are as per 99.5% high purity alumina[4] in the study. The Alumina is considered to be linear elastic[1#] with Young's modulus of 400GPa and a Poisson's ratio of 0.24 in the model. The temperature-dependent CTE of Alumina is shown in Figure 4.

Kovar (a trademark of CRS Holdings, Inc., Delaware) is a nickel-cobalt-ferrous alloy, which was originally designed to meet the requirement for a sound glass to metal seal required in electronic devices and high voltage insulators. As shown

1# Linear elastic: linear stress-strain failure at all strains; no plasticity

in Figure 4, the CTE of Kovar matches the CTE of Alumina up to ~400°C. Afterward, there is a significant expansion differential with the Alumina. Therefore, detailed data points of CTE to capture the transitional behavior are included in the FEA. For the analysis, the Kovar alloy is modeled as an elastic material with Young's modulus of 138 GPa and a Poisson's ratio of 0.317.[5]

The brazing alloy, TiCuSil, is considered to be perfectly plastic. A rate-independent constitutive plasticity theory[6] is used for brazing alloy with non-linear isotropic hardening rule with associated Von-Mises yield criteria. The brazing material is included in the model because its plastic behavior tends to relieve some of the internal stresses in the brazed joint during the cooling phase. Bilinear isotropic hardening data,[7] used in the analysis, are shown in Figure 5.

Analysis Settings and Loads

The implemented simulation methodology consists of an isothermal cool-down load step approach (e.g., 780°C → ambient), as shown in Figure 6. The zero strain temperature for the FEA is assigned as 780°C as shown in Figure 7. This assignment of boundary condition ensures no residual strain would be present in the brazed joint during the start of cool down. The assembly is then allowed to cool down isothermally to the room temperature. The isothermal approximation can be discerned as the assembly is having high thermal diffusivity and small size. As the brazing material causes non-linearity in the analysis, therefore non-linearity attributes are used for the solution.

Frictionless support is provided at the bottom of the assembly, as shown in Figure 8. This 2D geometry is in the

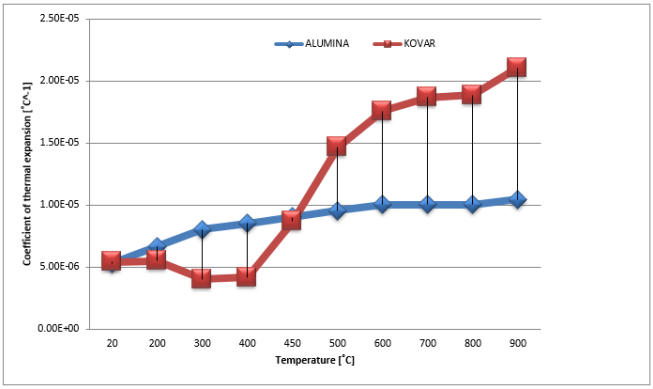

Figure 4: Instantaneous coefficient of thermal expansion for Alumina and Kovar

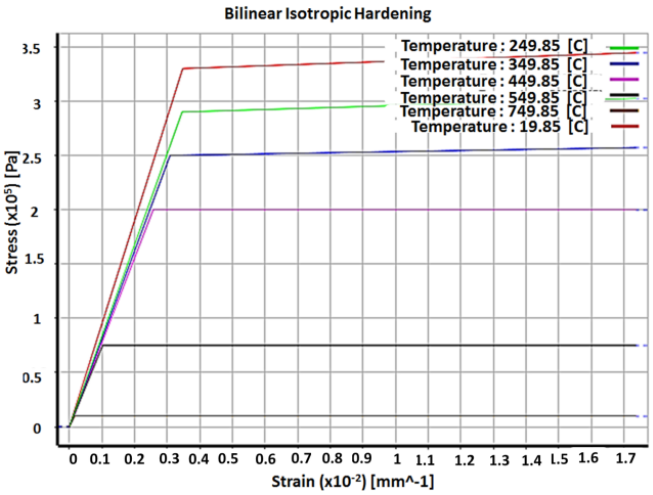

Figure 5: Bilinear isotropic hardening data for TiCuSil

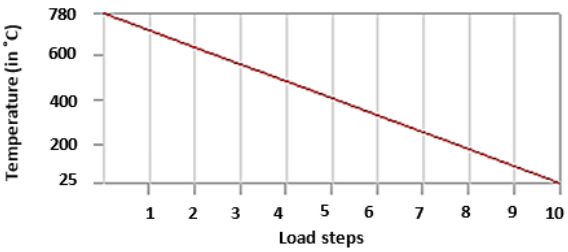

Figure 6: Load steps from 780°C to ambient

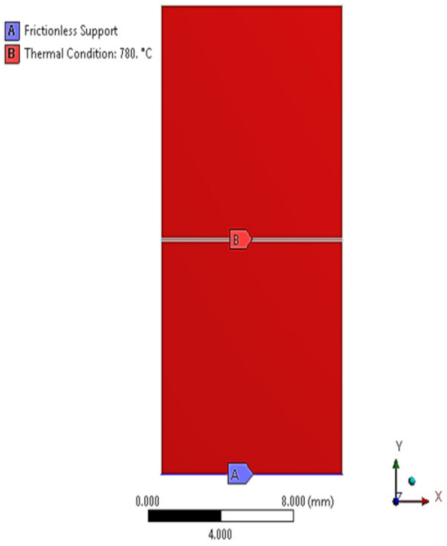

Figure 7: Boundary conditions and loads

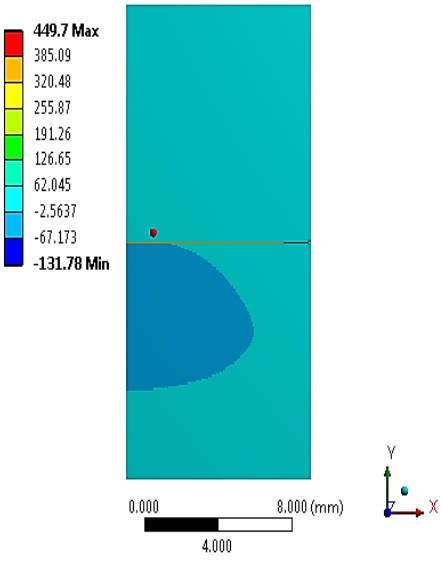

Figure 8: ANSYS result of the assembly

XY plane, where Y is the axis of symmetricity, and hence, it is allowed to expand or contract in XY plane on the frictionless support.

FEA Results

The simulation implies that the maximum tensile stress of 449.7 MPa is generated in the brazed part of the assembly, as shown in Figure 9. Due to high non-linearity involved at the corner of the brazed junction, as the material properties are changing significantly, stress concentration is observed.

The maximum residual stresses developed in the FE model changes with time, as shown in Figure 10. It can be observed from the graph that the slope of residual stresses has three distinctive zones. Zone 1 shows a steep rise in the residual stresses until 4.4 seconds. In zone 2, the residual stresses are dipping whereas, in zone 3, residual stresses start increasing again but at a slower pace. This behavior of steep rise, dipping, and increment at a slower pace again can be understood from the CTE graph of Kovar and Alumina, in which it can be seen that the CTE values have big mismatch for zone 1, close match of CTE in zone 2, and relatively less mismatch in zone 3.

To check the membrane and bending stresses, developed in the model, linearization of the stresses is carried out. The linearization result for brazing material is shown in Figure 11. Membrane stress is 362 MPa, and the maximum bending stress is 21.7 MPa.

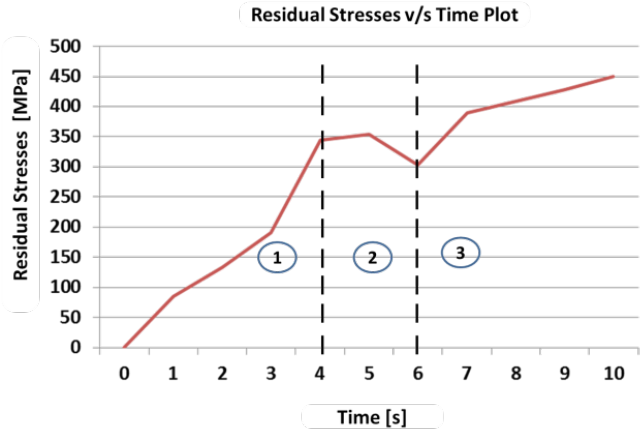

Figure 9: Residual stresses *vs.* time plot

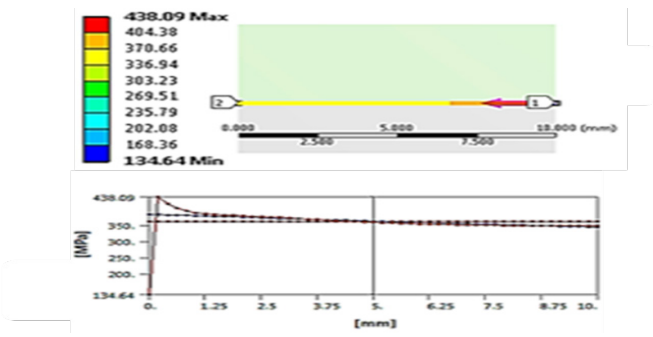

Figure 10: Linearization of stresses for brazing material

In ceramic material, maximum tensile stress is 328.87 MPa, and maximum compressive stress is 131.78 MPa, as shown in Figure 12.

Linearization of the result for the ceramic material is checked, and the results are shown in Figure 13. Membrane and membrane plus bending stresses are 5.6 and 21.96 MPa, respectively.

In Kovar the maximum tensile stress generated is 84.8 MPa, and the maximum compressive stress is 93.9 Mpa, as shown in Figure 14.

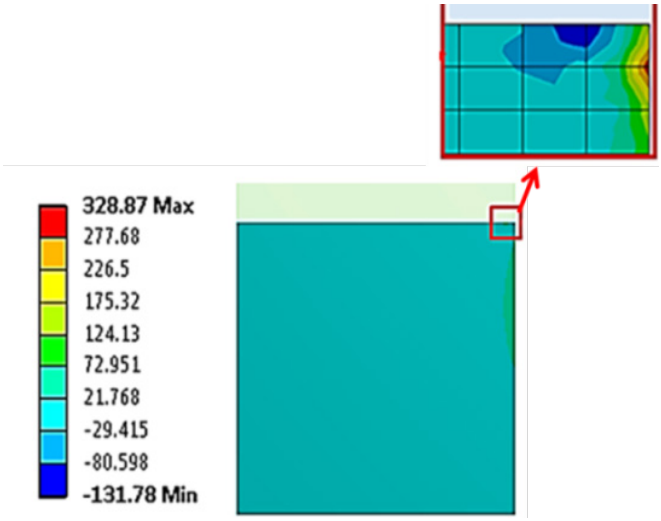

Figure 11: ANSYS result for ceramic part

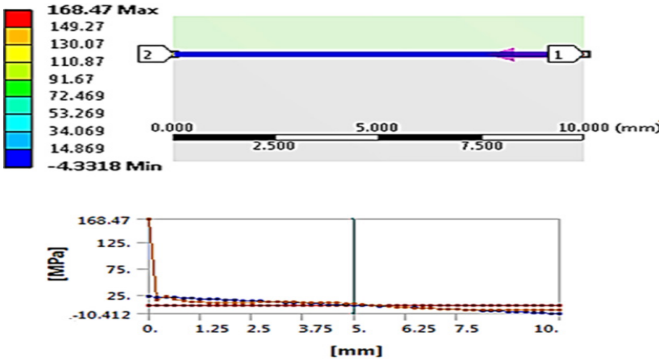

Figure 12: Linearization of stresses for ceramic

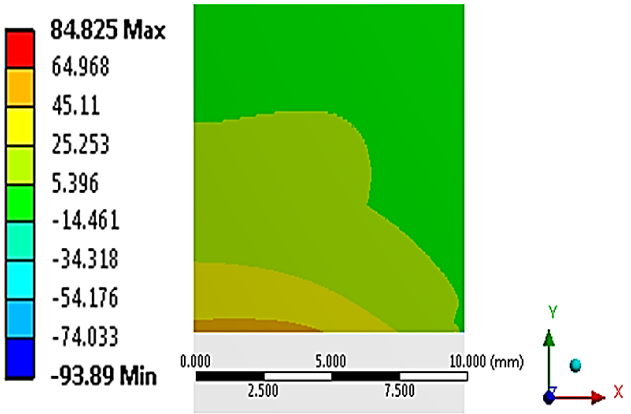

Figure 13: ANSYS result for Kovar part

American Society of Mechanical Engineers Code (ASME) Validation of the Results

The results of residual stresses are verified with the ASME code.[8] In the ASME code, stresses are mainly divided into two categories primary stresses and secondary stresses.

In this case, where thermal loading is applied, metallic parts will be subject to secondary stresses only. The allowable stress limit for the secondary stresses is:

$$Q = (Qm + Qb) < 3Sm \quad (1)$$

Where, Q is the secondary stress, which consists of the secondary membrane (Qm) and the bending (Qb) stresses, in the metal part and Sm is the allowable membrane stress of the material.

Whereas, in the ceramic material, which is a brittle material that does not undergo the plastic deformation, all the stresses developed are considered as primary stresses, and hence the limit is taken the same as used for comparison of primary stresses.

The stresses for different parts are summarized in Table 1 and found within the allowable limit. For metals, the results comply with ASME, whereas for non-metallic parts, the allowable limit is considered with respect to flexural strength,[9] and factor of safety (FOS) = 5 is adopted for the allowable stresses.

Sample Manufacturing

Alumina and Kovar disks of dimensions 20 mm diameter and 10 mm height of each were prepared. A foil of TiCuSil was placed in between the Alumina and Kovar disks. Brazing of Alumina Kovar sample was carried out in the vacuum brazing furnace using the thermal cycle, as shown in Figure 15. The test sample was brazed successfully without any visual surface cracks in the hoop direction, as shown in Figure 16.

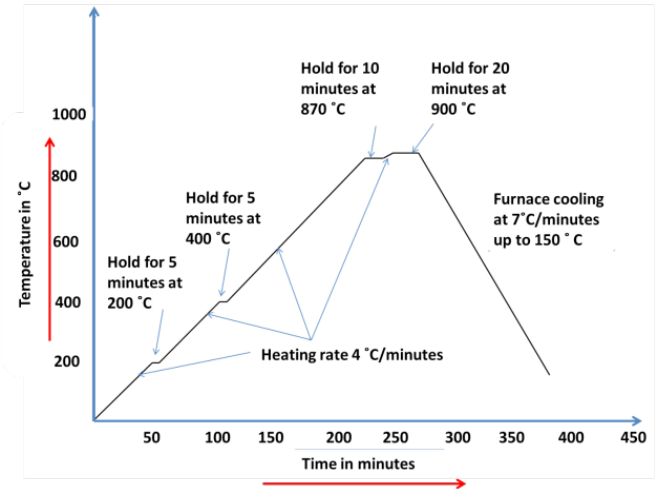

Figure 14: Thermal cycle for the brazing process

Table 1: Stress results in different parts of the assembly

Member	*Membrane (MPa)*	*Membrane + bending (MPa)*	*Allowable limit (MPa)*
Alumina	5.6	21.96	74
Brazing alloy	365.14	394.18	542
Kovar	36.4	72.9	516

Residual Stress Measurement Using XRD

Two techniques for residual stress measurement are identified. They are (1) X-ray diffraction (XRD) method, and (2) drilling hole strain gauge method (ASTM E 837-08). In this work, the XRD technique of residual stress measurement is used, which works on Bragg's law. In this method, the elastic strain is measured using Bragg's law, and calculation of the stress is done with Hooke's law together with the elastic modulus (E) and Poisson's ratio (v).

For the measurement, Xstress 3000 G2 machine from Stresstech, as shown in Figure 16, is used for the analysis. This is a portable, versatile machine that is used for residual stress measurement in the material. It measures the absolute stress without the need for an unstressed sample for calibration.

The $\sin^2\Psi$ technique[10] of surface residual stress measurement using XRD is used. In this technique, interplanar distance "d" in a lattice is measured at different "Ψ" tilts, which is the angle between the normal of the surface and the incident and diffracted beam bisector, of the sample. Using the interplanar lattice spacing and multiple Ψ tilts data, a straight line is fitted by the least-squares regression, and the stress is calculated from the slope of the best fit line using Eq. 2.

$$\sigma_{\emptyset} = \left(\frac{E}{1+\vartheta}\right)_{(hkl)} \frac{1}{d_{\emptyset 0}} \left(\frac{\partial d_{\emptyset\Psi}}{\partial \sin^2\Psi}\right) \quad (2)$$

Where, $\sigma_{\emptyset}$ is stress in the sample at an angle Ø from the principal stress, E is Young's modulus of the material, ϑ is Poisson's ratio, h, k, and l are Miller indices, $d_{\emptyset 0}$ is lattice

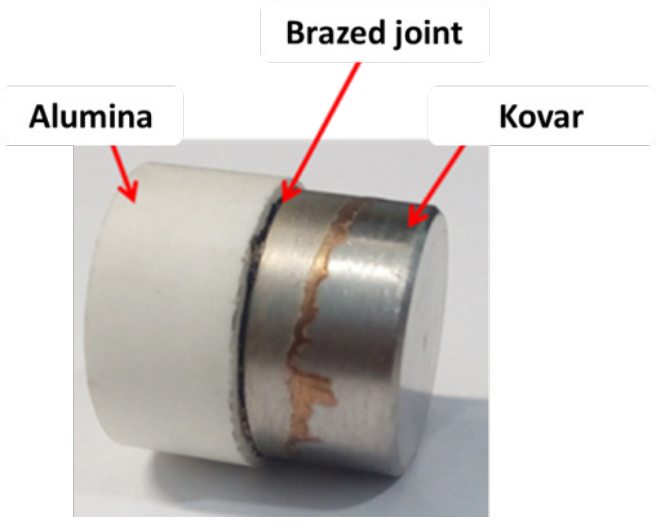

Figure 15: Brazed Alumina-Kovar sample

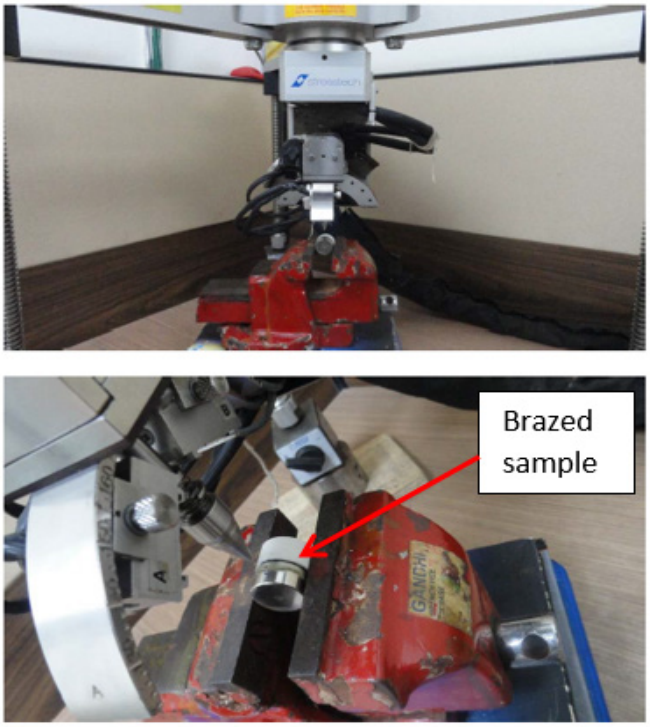

Figure 16: XRD of brazed sample

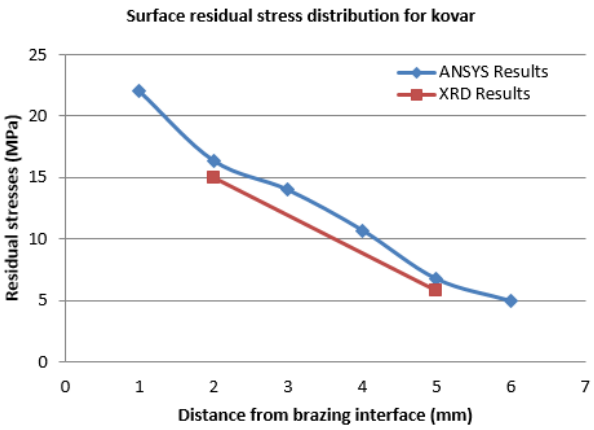

Figure 17: Surface residual stresses distribution in Kovar

spacing at Ø and 0° tilt angle, and $d_{\emptyset\psi}$ is lattice spacing at Ø and Ψ tilt angle.

The machine parameters used for the experiment are provided in Table 2.

The measurements at the sample are carried out at two spots. One is at 2 mm, and another is at 5 mm from the brazed junction in the Kovar material. The results of measured residual stresses are provided in Table 3.

The experimental and FEA results show the percentage deviation of 9.3 and 15.5% at 2 and 5 mm spots, respectively, which indicates the close compliance of both approaches. The minor difference between the values of FEA and XRD could be attributed to (1) the differences in the material properties used from literature for the analysis and the material properties of actual materials used for XRD, (2) practical limitation of the exact marking of 2 and 5 mm spots for the measurement which may be affected by the brazing interface thickness by 100 microns, and (3) effect of the number of data points for d *vs.* $\sin^2\Psi$ chart, collection time, cleaning of the sample during XRD. Surface residual stresses distribution in analyzed cases using ANSYS and measured case using XRD is shown in Figure 17.

Table 2: X-ray diffraction (XRD) parameters for residual stress measurement

S. No.	*Parameters*	*Values*
1.	Radiation	CrKα
2.	2θ	149.0°
3.	Spot size	1 mm
4.	Exposure time	40 s, 4/4 tilts, 40/40° psi angles
5.	Young's modulus	138 GPa
6.	Poisson's ratio	0.3
7.	Calculation	Cross-correlation, constant background
8.	Measurement method	Modified d ($\sin^2\Psi$)

Table 3: Results of X-ray diffraction (XRD) and ANSYS at two spots

Residual stresses at 2 mm spot		*Residual stresses at 5 mm spot*	
XRD result (MPa)	*ANSYS result (MPa)*	*XRD result (MPa)*	*ANSYS result (MPa)*
15	16.4	5.8	6.7

Conclusion

To understand the residual stress characteristics during the brazing process in the dissimilar materials, due to the fact of the large variation in their CTEs for a long temperature range, a detailed FE analysis has been carried out. Temperature-dependent non-linear material properties have been applied to get realistic results. Further, experimental validation on the manufactured sample has been carried out using XRD based residual stress measurement technique at two spots. It is assessed that the FEA results of brazed joint residual stresses are in good agreement with the experimental XRD measurement.

Future studies will focus on the FEA of the ceramic feedthroughs designed for the different shapes and sizes. As the shape and size change, the behavior of residual stresses also changes for the brazed joints and, therefore, becomes the important aspect of physical the residual stresses by modifications in the design as needed.

Acknowledgment

The authors would like to acknowledge Thyagarajan R. and Nitin Kanoongo from NFTDC, Hyderabad, for Kovar and braze alloy material, and preparing the brazed sample at their facility.

References

[1] ITER Organization. (2020). *What is ITER*. Retrieved 2020, from https://www.iter.org/proj/inafewlines.

[2] AWS. (1976). *Brazing Manual* (3 ed.). American Welding Society.

[3] Lugscheider, E. & Tillman, W. (1993). Methods for Brazing Ceramic and Metal-Ceramic Joints. *Materials and Manufacturing Processes*, 8 (2), 219-238.

[4] Auerkari, P. (1996). *Mecahnical and Physical Properties of Engineering Alumina Ceramics.* Espoo: VTT Offsetpaino, Finland.

[5] ASTM International. (2013). ASTM F15-04: *Standard Specification for Iron-Nickel-Cobalt Sealing Alloy.* American Society for Testing and Materials.

[6] ANSYS Inc. (2012). *Rate Independent Plasticity.* ANSYS Mechanical Basic Structural Nonlinearities.

[7] Neilsen, M.K., Stephens, J.J. & Gieske, J.H. (1996). *A Viscoplastic Theory for Braze Alloys*, Sandia Report, SAND-96-0984.

[8] ASME. (2010). BPVC-VIII-2: *Boiler Pressure Vessel Code Section VIII-Rules for Construction of Pressure Vessels Division 2-Alternative Rules*. American Society for Mechanical Engineers

[9] IEC. (1997). IEC 60672-3: *Ceramic and Glass-Insulating Materials, Part 3: Specifications for individual materials*. International Electrotechnical Commission.

[10] Paul, S.P. (1986). *X-Ray Diffraction Residual Stress Technique.* Metals Handbook. 10. Metals Park: American Society for Metals, 380-392